

## Positron impact ionization of atomic hydrogen at low energies

K CHAKRABARTI

Department of Mathematics, Scottish Church College, 1 & 3 Urquhart Square, Calcutta 700 006, India

MS received 26 June 2000

**Abstract.** Low energy positron impact ionization of atomic hydrogen is studied theoretically using the hyperspherical partial wave method of Das [1] in constant  $\Theta_{12}$ , equal energy sharing geometry. The TDCS reveal considerable differences in physics compared to electron impact ionization under the same geometry.

**Keywords.** Hyperspherical; partial wave; collision; ionization; cross section.

PACS No. 34.85.+x

### 1. Introduction

The study of low energy ionization of atomic hydrogen has undergone a rapid development in the past few years. Three distinct theories for describing low energy ionization can now be identified: (i) distorted wave theories (Jones *et al* [2], Röder *et al* [3]), (ii) methods based on modification of the BBK technique [4] by introduction of effective charges (Berakdar and Briggs [5], Berakdar [6]), (iii) close coupling methods (Bray and Stelbovics [7], Bray *et al* [8], Kato and Watanabe [9], Das [10], Das and Chakrabarti [11]). All these methods have been used to calculate triple differential cross sections (TDCS) for low energy electron impact ionization successfully. In particular, the close coupling calculations of Bray and Stelbovics [7] and that of Kato and Watanabe [9] describe the total ionization cross section from near threshold to about 500 eV very accurately.

Due to lack of experimental data, the study of positron impact ionization is till now only of limited interest. However, it is interesting to investigate the differences in physics of positron and electron impact ionization. Such comparisons have been undertaken before, particularly in the intermediate energy range for Ehrhardt asymmetric kinematics by Joachain and Piraux [12], Brauner *et al* [4], Das *et al* [13]. The results exhibit typical binary-recoil peak structure, characteristic of electron impact ionization, with peak positions shifted towards smaller deflection angles.

We present here a study of low energy positron impact ionization, a nearly unexplored area, in the equal energy sharing, constant  $\Theta_{12}$  geometry, where the angular separation  $\Theta_{12}$  between the emerging particles is kept constant.

## 2. Theory

The hyperspherical partial wave method of Das [1] is used here to compute the TDCS. The procedure has been used before to study electron impact ionization for different kinematic conditions by Das and Chakrabarti [11,14] under the *weak correlation approximation* which neglects coupling among various partial waves in the final channel (see [11] for details). The method works best when the final channel post collision interaction is weak, a condition satisfied for constant  $\Theta_{12}$  geometries with large  $\Theta_{12}$ . We therefore restrict ourselves to equal energy sharing, constant  $\Theta_{12}$  geometries at 30 eV and 20 eV impact energies. Another reason for choosing this geometry and impact energy is that it will allow us to compare the present results with the results of electron impact ionization in our previous work [11].

The computational procedure is the same as our work [11] with the interaction potential  $V$  replaced by

$$V = -\frac{1}{r_{12}} + \frac{1}{r_2}, \quad (1)$$

where  $\vec{r}_1, \vec{r}_2$  are respectively the coordinates of the bound and projectile particles. Also as the particles involved in the final state are not identical we do not take exchange contributions to the TDCS.

## 3. Results and discussion

The results in figure 1 are for an incident energy 30 eV and angular separation  $\Theta_{12} = 90^\circ$  (a),  $120^\circ$  (b),  $150^\circ$  (c) and  $180^\circ$  (d). For a head on collision, the incoming positron would tend to pull the atomic electron backward. Consequently there would be more backward scattering events than forward ones. This is clearly exhibited in figure 1d where the TDCS peaks near  $180^\circ$  and dips at  $0^\circ$ . The symmetry in the TDCS occurs here due to the choice  $\Theta_{12} = 180^\circ$  which leads to a symmetric configuration. For ionization with electrons, the incoming electron tends to push the atomic electron to the far side, causing preferential ejection around the forward direction. Scattering in the directions  $90^\circ$  and  $270^\circ$  is minimum leading to dips in the TDCS near these scattering angles. We find this to be true from figure 1d of ref. [11]. (Note that though in ref. [11] we have results up to  $\Theta_{12} = 150^\circ$ , the  $\Theta_{12} = 180^\circ$  case, needed for comparison, is similar to  $\Theta_{12} = 150^\circ$ ).

When the angular separation is decreased progressively from  $150^\circ$  to  $90^\circ$ , the attraction between the positron and electron causes asymmetry in the TDCS. We now find two peaks, one near the forward direction and the other (which is smaller) near the backward direction (see figure 1a–c). For ionizations by electrons in a similar situation the TDCS retains symmetry about the directions  $\Theta_{12}/2$  and  $\pi + \Theta_{12}/2$  for all  $\Theta_{12}$  (see figure 1a–d) of [11]. This symmetry is due to the presence of two identical particles in the final state.

The position of the peaks can be linked to the momentum transfer  $\vec{t} = \vec{k}_i - \vec{k}_2$ . In this work we use the suffix  $i$  for the incident particle while the suffixes 1 and 2 are respectively used for the *ejected* and *scattered* particles. The direction of momentum transfer  $\theta_t = \cos^{-1}(\hat{t} \cdot \hat{k}_i)$  reaches a maximum  $\theta_{t_{\max}}$  (with respect to  $\theta_2$ ) which is approximately  $31.5^\circ$  for an incident energy 30 eV. A peak in the cross section occurs in the direction

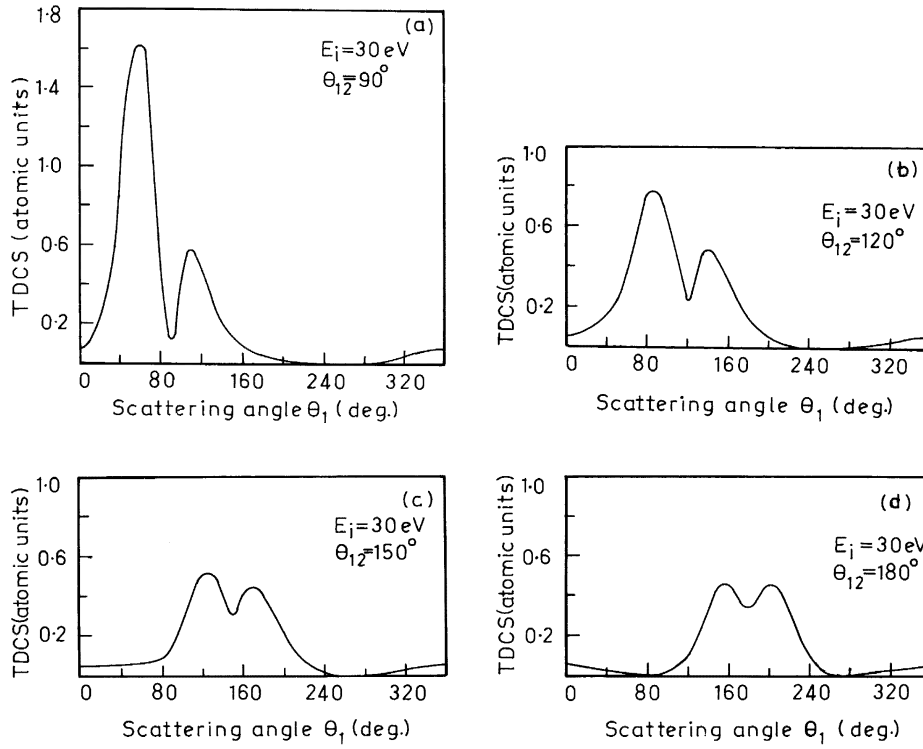


**Figure 1.** TDCS versus ejection angle for positron impact ionization of atomic hydrogen in constant  $\Theta_{12}$ , equal energy sharing geometry for an incident energy  $E_i = 30$  eV. Theory: Continuous curve, present results.

$\theta_1 = \Theta_{12} - \theta_{t \max}$ . We shall see that this peak is primarily due to binary positron-electron scattering. The second peak occurs approximately in the direction  $\theta_1 = \Theta_{12} + \theta_{t \max}$  and its origin can be traced to a recoil ionization process. It is interesting to note that the corresponding peaks for ionization by electrons occur at  $\theta_{t \max}$  and  $\Theta_{12} + \theta_{t \max}$ .

To analyse the origin of the peaks, following Berakdar *et al* [15] we write the  $T$ -matrix as

$$T = \langle \Psi_f^{(-)} | -\frac{1}{r_{12}} + \frac{1}{r_2} | \Phi_i \rangle = T_{e+e} + T_{e+N}, \quad (2)$$

where  $T_{e+e}$  correspond to positron-electron scattering and  $T_{e+N}$  correspond to positron-nucleus scattering. Separate contributions of  $T_{e+e}$  and  $T_{e+N}$  are plotted in figure 2 for  $\Theta_{12} = 90^\circ$  (a) and  $\Theta_{12} = 180^\circ$  (b). In both figures it is clear that positron-nucleus scattering dominates the peak near  $180^\circ$ . Due to reasons outlined before the forward peak is absent when  $\Theta_{12} = 180^\circ$  (figure 2b). For  $\Theta_{12} = 90^\circ$  positron-electron scattering contributes mainly to the forward peak as can be seen from figure 2a. It appears that recoil ionization process is responsible for the backward peak, while the forward peak is largely due to binary positron-electron scattering.

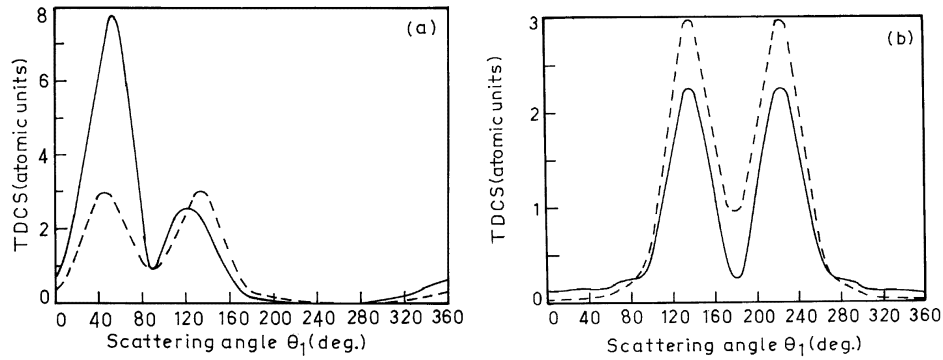


**Figure 2.** Separate contributions of the positron-electron amplitude  $T_{e+e}$  and positron-nucleus amplitude  $T_{e+N}$  (see text for details) plotted against ejection angle  $\theta_1$  for  $E_i = 30$  eV and (a)  $\Theta_{12} = 90^\circ$ , (b)  $\Theta_{12} = 180^\circ$ . Theory: Solid line – TDCS calculated with  $T_{e+e}$  only; dashed line – TDCS calculated using  $T_{e+N}$  only.

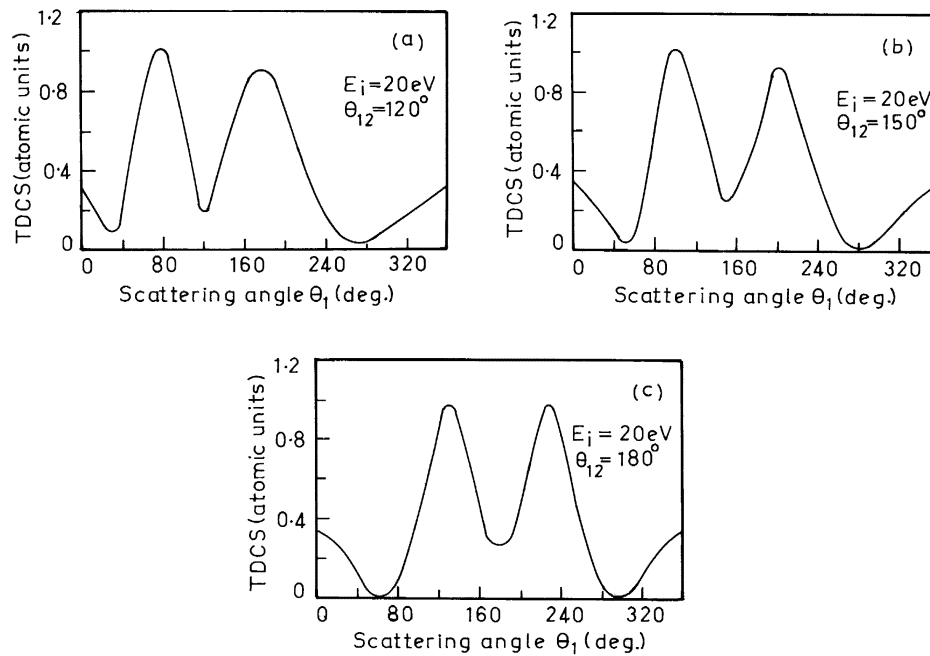


**Figure 3.** Same as figure 1 except for  $E_i = 20$  eV.

Figure 3 presents results for an incident energy 20 eV and (a)  $\Theta_{12} = 120^\circ$ , (b)  $\Theta_{12} = 150^\circ$  and (c)  $\Theta_{12} = 180^\circ$ . Unlike the 30 eV case, the TDCS curves do not show an appreciable change in shape as  $\Theta_{12}$  is decreased from  $180^\circ$  to  $120^\circ$ . In this case  $\theta_{t \max}$  is approximately  $23.5^\circ$ . Surprisingly the peaks in the TDCS no longer occur near the

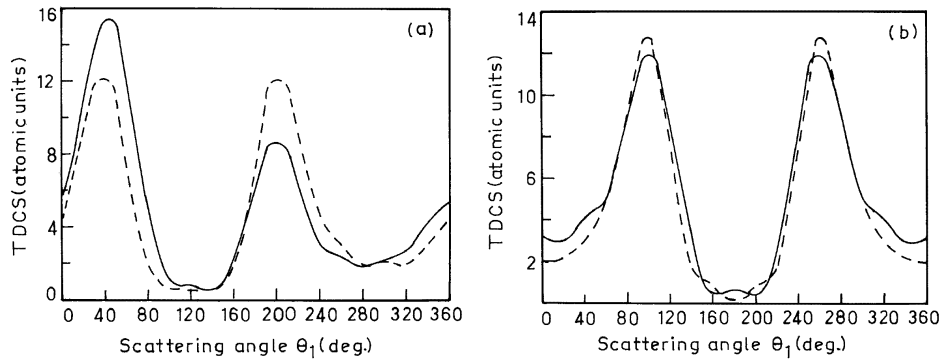


**Figure 4.** Same as figure 2 except for  $E_i = 20$  eV and (a)  $\Theta_{12} = 120^\circ$  and (b)  $\Theta_{12} = 180^\circ$ .

directions  $\Theta_{12} \pm \theta_{l \max}$  but are considerably shifted away from these directions. Stronger attraction at lower energies between the emerging particles is probably responsible for this behaviour. Once again we plot the contributions of  $T_{e^+e}$  and  $T_{e^+N}$  to the TDCS in figure 4 for  $\Theta_{12} = 120^\circ$  (a) and  $\Theta_{12} = 180^\circ$  (b). From figure 4b we find that there is no clear evidence that the backward peak for  $\Theta_{12} = 180^\circ$  is due to positron-nucleus scattering. Rather both positron-nucleus and positron-electron scattering contribute equally to the backward peak. For a smaller angular separation, e.g.  $\Theta_{12} = 120^\circ$  (figure 4a), the backward peak is again dominated by positron-nucleus scattering while positron-electron scattering contributes mainly to the forward peak.

#### 4. Conclusion

To conclude, we have analysed positron hydrogen atom ionization collision at low energies in constant  $\Theta_{12}$  geometry. An attempt is made to trace the position and origin of the peaks in TDCS. The forward peak is shown to be largely due to binary positron-electron scattering. At 30 eV, dominant contribution to the backward peak comes from positron-nucleus scattering. At lower energies both positron-electron and positron-nucleus scattering contribute equally to the backward peak.

#### Acknowledgement

I am grateful to Prof. J N Das for helpful discussions and for his suggestions on improvement of the manuscript.

#### References

- [1] J N Das, *Aust. J. Phys.* **47**, 743 (1994)
- [2] S Jones, D H Madison, A Franz and P L Altick, *Phys. Rev.* **A48**, R22 (1993)

- [3] J Röder, J Rasch, K Jung, Colm T Whelan, H Ehrhardt, R J Allan and H R J Walters, *Phys. Rev.* **A53**, 226 (1996)
- [4] M Brauner, J S Briggs and H Klar, *J. Phys.* **B22**, 2265 (1989)
- [5] J Berakdar and J S Briggs, *Phys. Rev. Lett.* **72**, 3799 (1994)
- [6] J Berakdar, *Phys. Rev.* **A53**, 2314 (1996)
- [7] I Bray and A T Stelbovics, *Phys. Rev. Lett.* **70**, 6746 (1993)
- [8] I Bray, D A Konovalov, I E McCarthy and A T Stelbovics, *Phys. Rev.* **A50**, R2818 (1994)
- [9] D Kato and S Watanabe, *Phys. Rev. Lett.* **74**, 2443 (1995)
- [10] J N Das, *Pramana – J. Phys.* **50**, 58 (1998)
- [11] J N Das and K Chakrabarti, *Phys. Rev.* **A56**, 365 (1997)
- [12] C J Joachain and B Piraux, *Comm. At. Mol. Phys.* **17**, 261 (1986)
- [13] J N Das, A Dey and K Chakrabarti, *Pramana – J. Phys.* **45**, 41 (1995)
- [14] J N Das and K Chakrabarti, *Pramana – J. Phys.* **47**, 249 (1996)
- [15] J Berakdar, J Röder, J S Briggs and H Ehrhardt, *J. Phys.* **B29**, 6203 (1996)